Importance of tropospheric $ClNO_2$ chemistry across the Northern Hemisphere

Golam Sarwar[1,*], Heather Simon[2], Jia Xing[1], Rohit Mathur[1]

[1]National Exposure Research Laboratory, U.S. Environmental Protection Agency, RTP, NC

[2]Office of Air Quality Planning and Standard, U.S. Environmental Protection Agency, RTP, NC

[*]Correspondence to Golam Sarwar: sarwar.golam@epa.gov

Key Points

1. Heterogeneous nitryl chloride chemistry is implemented into a hemispheric model
2. The largest enhancements of nitryl chloride occur over China and Western Europe
3. Nitryl chloride subsequently affects tropospheric chemistry

Abstract

Laboratory and field experiments have revealed that uptake of dinitrogen pentoxide (N_2O_5) on aerosols containing chloride produces nitryl chloride ($ClNO_2$) and nitric acid. We incorporate heterogeneous $ClNO_2$ formation into the hemispheric Community Multiscale Air Quality model. This heterogeneous chemistry substantially enhances $ClNO_2$ levels in several areas of the Northern Hemisphere and alters the composition of airborne reactive nitrogen, comprising more than 15% of monthly-mean values in some areas. Model results suggest that this heterogeneous chemistry reduces monthly-mean total nitrate by up to 25% and enhances monthly-mean daily maximum 8-hr ozone by up to 7.0 ppbv in some areas. The pathway also enhances hydroxyl radical by more than 20% in some locations which in turn increases sulfate and other secondary pollutants. The largest $ClNO_2$ concentrations and impacts occur over China and Western Europe, two areas in which few relevant field measurements have been made.

Index Terms: 0478 **-** Pollution: urban, regional and global, 0340 - Middle atmosphere: composition and chemistry, 0305 - Aerosols and particles

1. Introduction

Nitryl chloride ($ClNO_2$) builds up in the boundary layer at night and subsequently undergoes photolysis in the morning to produce chlorine radicals ($Cl^{\cdot}$) and nitrogen dioxide (NO_2). Consequently, $ClNO_2$ has been shown to be both an important radical source [*Osthoff et al.,* 2008*; Thornton et al,* 2010*; Phillips et al.,* 2012*; Reidel et al.,* 2012*; Young et al.,* 2012] and an important component of total reactive nitrogen (NO_Y) [*Osthoff et al.,* 2008*; Thornton et al,* 2010*; Mielke et al*., 2011*; Sarwar et al.,* 2012*; Mielke et al.,* 2013]. One study found that under certain ambient early-morning conditions, more chlorine radicals are formed from $ClNO_2$ photolysis than the hydroxyl radicals (HO) formed from ozone (O_3) photolysis [Phillips et al., 2012]. Another study suggests that $ClNO_2$ photolysis may produce more radicals than nighttime nitrous acid formation and its subsequent photolysis in the morning [Young et al., 2012]. Chlorine radicals react with organic compounds leading to O_3 production. NO_2 cycled through $ClNO_2$ also leads to O_3 production. Thus, elevated atmospheric $ClNO_2$ enhance O_3 production in the atmosphere as shown in by *Simon et al*. [2009] and *Sarwar et al.* [2012].

Laboratory studies suggest that $ClNO_2$ forms from the uptake of dinitrogen pentoxide (N_2O_5) on aerosols containing chloride [*Bertram and Thornton*, 2009 and *Roberts et al*., 2009]. Traditionally, the uptake of N_2O_5 on aerosols was believed to primarily produce nitric acid (HNO_3). Consequently the $ClNO_2$ chemical pathway can affect total nitrate ($TNO_3 = HNO_3$ + particulate nitrate) as shown by *Sarwar et al.* [2012].

Osthoff et al. [2008] first measured atmospheric $ClNO_2$ in 2006 and reported a peak value of about 1.2 ppbv near Houston, Texas. *Reidel et al.* [2012] also reported elevated levels of $ClNO_2$ in Los Angeles, California. Other investigators have also found substantial ambient

concentrations of $ClNO_2$ in areas distant from marine influence [*Thornton et al.,* 2010*; Mielke et al.,* 2011*; Philips et al.,* 2013; *Reidel et al.,* 2013].

While there are a growing number of studies which have measured ambient $ClNO_2$ concentrations and studied both its formation and its impact on tropospheric chemistry, most have been conducted in locations throughout North America including Houston [*Osthoff et al*., 2008], Los Angeles [*Reidel et al*., 2012; *Meilke et al*., 2013], Colorado [*Thornton et al*., 2010, *Reidel et al.,* 2013], Long Island Sound [*Kercher et al*., 2009] and Calgary [*Mielke et al.,* 2011]. A limited number of photochemical modeling studies have also focused on North America [*Simon et al*., 2009; *Simon et al*., 2010; *Sarwar et al.*, 2012]. Only two measurement studies and no modeling studies have examined effects of tropospheric $ClNO_2$ chemistry outside of North America: one study in the North Atlantic [*Kercher et al*., 2009] and one in Frankfurt, Germany [*Phillips et al.*, 2013]. Photochemical models provide a means to examine chemistry over much larger spatial extents than is feasible with specialized measurement studies and can identify times and locations where $ClNO_2$ is most likely to play an important role in radical chemistry and nitrogen oxides (NO_x) cycling. In this work, for the first time, we assess the importance of the heterogeneous $ClNO_2$ production on tropospheric chemistry across the Northern Hemisphere (NH).

2. Method

2.1 Model description and application

The study uses the CMAQ model (version 5.0.2) to assess the impacts of $ClNO_2$ on air quality. The details of CMAQ have been described elsewhere [*Foley et al.,* 2010; *Byun and Schere*, 2006; *Binkowski and Roselle*, 2003]. Many studies have demonstrated the skill of the CMAQ model in simulating air quality [*Eder and Yu*, 2006; *Appel et al*., 2007; *Appel et al*., 2008;

Sarwar et al., 2008; *Foley et al.*, 2010; *Appel et al.*, 2012; *Sarwar et al.*, 2013; *Sarwar et al.*, 2014]. The horizontal extent of the modeling domain covered the entire NH and was discretized using a grid of 108-km resolution using a polar stereographic coordinate system while the vertical extent of the model extended from surface to 5 kPa and contained 44 layers [*Mathur et al.*, 2011, 2013]. Meteorological fields for the study were prepared using the Weather Research and Forecasting (version 3.3) model [*Skamarock et* al., 2008]. Model simulations were conducted for two months in winter (Dec 2005-Jan 2006) and two months in summer (May-Jun 2006). The first month in each season was used as spin-up period; results for the subsequent months in winter and summer are presented. Each simulation used the 2005 version of the Carbon Bond (CB05) chemical mechanism with updated toluene chemistry [*Whitten et al.*, 2010]. The reaction mechanism also included gas-phase chlorine chemistry as well as the uptake of N_2O_5 on aerosols [*Sarwar et al.*, 2012]. The chlorine chemistry includes 25 gas-phase chemical reactions of $Cl\cdot$ with organic and inorganic species including the formation of the ClONO isomer from the reaction of NO_2 and $Cl\cdot$ [*Leu*, 1984] as well as the photolysis of $ClNO_2$. We expect ClONO and $ClNO_2$ to behave similarly so we use $ClNO_2$ to represent both in the model. Two different simulations were performed for each time period as follows. In the first simulation, the uptake of N_2O_5 on aerosols only produced HNO_3. In the second simulation, the heterogeneous formation of $ClNO_2$ was turned on; thus, the uptake of N_2O_5 on aerosols containing chloride produced both HNO_3 and $ClNO_2$. The difference in the model results were attributed to the heterogeneous $ClNO_2$ formation chemistry.

The study uses anthropogenic emissions from the Emissions Database for Global Atmospheric Research (http://edgar.jrc.ec.europa.eu/index.php) and biogenic emissions from Global Emissions InitiAtive (http://www.geiacenter.org). The model includes two major sources of particulate chloride: sea salts and biomass burning. The CMAQ model uses the

parameterization of *Gong* [2003] for calculating sea salt emissions [*Kelly et al.*, 2010]. Emissions of particulate chloride from biomass burning activity were based on *Lobert et al.* [1999]. These biomass burning emissions include the following source categories: savanna fires, wood and charcoal burning, deforestation, agro-industrial and dung burning, forest wildfires, slash and burn/shifting cultivation, burning in the fields, shrubland, heath, tundra fires, and grassland fires [*Lobert et, al., 1999*]. These estimates likely represent the upper limit of the biomass burning emissions. However, many other sources including those of power generation emit particulate chloride [*Reff et al., 2009*]. Global emissions estimates of these other sources are not currently available and consequently are not included in this study. Thus, the results presented herein do not reflect the full impact of the $ClNO_2$ chemistry since particulate chloride emissions from industrial sources are not included. The CMAQ model uses three modes to describe the aerosol size distribution: Aitken mode, accumulation mode, and coarse mode. Sea salt emissions are apportioned into accumulation mode and coarse mode particles while biomass burning emissions are apportioned only into accumulation mode particles. Calculated sea salt derived accumulation mode particulate chloride emissions for the NH are 1.6 Tg in January and 0.77 Tg in June while sea salt derived coarse mode particulate chloride emissions are 102 Tg in January and 46.6 Tg in June. Accumulation mode particulate chloride emissions from biomass burning are 0.4 Tg in January and 0.4 Tg in June. Sea salt contributes substantially more to the total particulate chloride emissions than biomass burning activity in coastal and marine environments.

2.2 Heterogeneous $ClNO_2$ formation chemistry

The standard CMAQv5.0.2 model includes the uptake of N_2O_5 on aerosols to produce HNO_3 as the only reaction product (R1). It uses the *Davis et al.* [2010] parameterization for the

heterogeneous uptake coefficient of N_2O_5 (γ_{N2O5}) and accounts for the heterogeneous conversion of N_2O_5 on Aitken mode and accumulation mode aerosols.

$$N_2O_5(g) + H_2O(aq) \rightarrow 2\ HNO_3(g) \quad \text{(R1)}$$

Finlayson-Pitts et al. [1989], *Bertram and Thornton* [2009], and *Roberts et al.* [2009] suggest that when particles contain chloride, the uptake of N_2O_5 also produces $ClNO_2$ as a reaction product (R2).

$$N_2O_5(g) + H_2O\ (aq) + Y\ Cl^-\ (aq) \rightarrow Y\ (HNO_3(g) + ClNO_2\ (g)) + 2(1 - Y)\ HNO_3\ (g) \quad \text{(R2)}$$

The yield of $ClNO_2$ (Y) depends on particulate chloride concentration [Cl^-] and particle liquid water content [H_2O(l)] and has been parameterized *by Bertram and Thornton* [2009] and *Roberts et al.* [2009] (Eq-1). *Bertram and Thornton* [2009] measured a constant of 483 while *Roberts et al.* [2009] measured a constant of 485 for use in Eq-1.

$$Y = \frac{1}{1+\frac{[H_2O(l)]}{483\ [Cl^-]}} \quad (1)$$

Bertram and Thornton [2009] also suggested that the presence of particulate chloride alters γ_{N2O5} and developed the following parameterization (Eq-2).

$$\gamma_{N_2O_5} = 3.2x10^{-8}k\left(1 - \frac{1}{\left(\frac{0.06\ [H_2O(l)]}{[NO_3^-]}\right)+1+\left(\frac{29\ [Cl^-]}{[NO_3^-]}\right)}\right) \quad (2)$$

Where [H_2O(l)] = particle liquid water (mol/L), [NO_3^-]= particulate nitrate (mol/L), [Cl^-] = particulate chloride (mol/L), and k represents the rate coefficient for the disassociation of N_2O_5 (aq) and is calculated as follows:

$$k = 1.15x10^6 - 1.15x10^6 e^{[-\ 0.13\ x\ [H_2O(l)]]} \quad (3)$$

158 *Betram et al.* [2009] compared the γ_{N2O5} parameterization from equation (2) to measurements
159 made on ambient aerosols and found that when organic content was low, relative humidity was
160 a primary controller of γ_{N2O5} while nitrate concentrations was a secondary controller. Since
161 the *Bertram and Thornton* [2009] parameterization does not explicitly account for the effects
162 of organics, the heterogeneous uptake coefficient may be over-estimated when organic aerosol
163 concentrations are high. The effect of not accounting for organic inhibition of N_2O_5 uptake
164 should be most pronounced in summer and less pronounced in winter. In this study, we replace
165 R1 with R2 in the CMAQ model and replace the *Davis et al.* [2010] parameterization with the
166 *Bertram and Thornton* [2009] formulation for γ_{N2O5}. The yields and heterogeneous uptake
167 coefficients are calculated separately on Aitken, accumulation, and coarse particles using Eq-
168 1 and Eq-2 respectively.
169
170 **3. Results and Discussion**
171
172 **3.1 Predicted $ClNO_2$ levels and the composition of total reactive nitrogen**
173 $ClNO_2$ forms at night and tends to peak before the sunrise. Predicted levels decrease rapidly
174 after sunrise and reach a minimum value during the day. Monthly mean of nightly 1-h
175 maximum $ClNO_2$ levels without and with the heterogeneous production are shown in Figure 1.
176 Predicted $ClNO_2$ levels formed via the gas-phase reaction of NO_2 + Cl are small (< 1 pptv) as
177 shown in Figure 1a and 1b. The inclusion of the heterogeneous formation reaction enhances
178 predicted $ClNO_2$ levels in many areas by more than three orders of magnitude. Collocation of
179 anthropogenic NO_x sources and particulate chloride from sea salt triggers the heterogeneous
180 production of $ClNO_2$ in coastal areas while NO_x and particulate chloride from biomass burning
181 activity activates the heterogeneous production of $ClNO_2$ over inland areas.
182

Predicted surface-level winter $ClNO_2$ values are greater than those in summer due to higher N_2O_5 levels, higher $ClNO_2$ yields, and lower mixing height. The colder winter temperature shifts the N_2O_5-NO_3 equilibrium towards N_2O_5 and the longer winter nights lead to more N_2O_5 accumulation in dark conditions. The monthly mean $ClNO_2$ yields range between 0.5-1.0 across most of the NH in winter, with values greater than 0.75 over the Oceans, China, parts of Africa, and the Southwestern United States. These high winter $ClNO_2$ yields and N_2O_5 concentrations lead to monthly mean nightly maximum winter $ClNO_2$ levels of more than 0.7 ppbv over large areas of China and Western Europe. The heterogeneous $ClNO_2$ formation pathway also produces more than 0.4 ppbv of winter $ClNO_2$ over parts of India, Western Europe, the Eastern United States and Southern California. In contrast, N_2O_5, $ClNO_2$ yields, and resulting $ClNO_2$ concentrations are lower in the summer. Monthly mean $ClNO_2$ yields range between 0-1.0 in the summer with values of 0.1-0.6 over Europe and the United States, and 0.5-1.0 over China. This results in summer $ClNO_2$ concentrations of up to 0.4 ppbv only over small areas of China and Western Europe. Predicted summer levels elsewhere in the NH are small compared to those obtained in winter. However, values greater than 200 pptv are predicted in some ares.

Predicted peak $ClNO_2$ levels from the current study are compared to the measured peak values from field studies in Table 1. While predicted winter levels tend to be closer to the observed data, summer levels are lower than the observations. Similar model calculations using the same chemistry but at a finer grid resolution (12-km) over the United States [Sarwar et al., 2012] predicted higher $ClNO_2$ concentrations (especially in the summer) which matched reasonably well with measurements in the United States suggesting that local peaks are likely smoothed out by the coarser grid resolution (108-km) used in this study. In addition, the coarse grid resolution may dampen localized O_3 titration due to artificial dilution of urban NO_x emissions

208 and thus could cause an underestimate of nighttime NO_3 and consequently N_2O_5 formation.
209 Therefore the modeling results presented here may not capture the largest $ClNO_2$ effects.
210
211 The heterogeneous production of $ClNO_2$ sequesters NO_x which would otherwise form HNO_3
212 and be lost quickly from the atmosphere via deposition. Upon sunrise $ClNO_2$ undergoes
213 photolysis liberating NO_x and $Cl^{\cdot}$, both of which affect atmospheric chemistry. The production
214 of $ClNO_2$ alters the relative composition of NO_Y. TNO_3 is the largest contributor to the NO_Y
215 budget in the model's surface layer and accounts for 54% and 51% of the total NO_Y in winter
216 and summer, respectively. NO_x is the second largest contributor to the NO_Y budget and
217 accounts for 23% of the total NO_Y in winter as well as in summer. In winter, nitrous acid
218 accounts for 0.2%, peroxyacetyl nitrate for 8.7%, higher peroxyacetyl nitrate for 5.8%, and
219 peroxynitric acid for 0.5% of NO_Y averaged over the entire NH. In contrast, $ClNO_2$ accounts
220 for 2.9% of NO_Y; thus, its contribution to NO_Y is more than that of nitrous acid or peroxynitric
221 acid and is half of the higher peroxyacetyl nitrate. In summer, nitrous acid accounts for 0.2%,
222 peroxyacetyl nitrate for 12.3%, higher peroxyacetyl nitrate for 7.8%, peroxynitric acid for
223 0.1%, and $ClNO_2$ for 0.1% of NO_Y averaged over the entire NH. Hence, summer $ClNO_2$ levels
224 are similar to those of peroxynitric acid. Thus, $ClNO_2$ accounts for a moderate fraction of the
225 NO_Y budget even when averaged over the entire NH. It, however, can comprise a larger fraction
226 of NO_Y in localized areas. For example, $ClNO_2$ accounts for more than 6% of winter NO_Y over
227 large areas of China and more than 15% of winter NO_Y in Scandinavia and northern Russia.
228 These seasonal and regional differences in the NO_Y composition then impact NO_X recycling in
229 the troposphere affecting both oxidant and particle formation as discussed next.
230
231 **3.2 Impact of the $ClNO_2$ production on total nitrate**

Figure 2 displays the monthly mean TNO_3 levels without the heterogeneous production of $ClNO_2$ and changes due to the heterogeneous $ClNO_2$ formation chemistry. Winter TNO_3 levels without the heterogeneous $ClNO_2$ formation chemistry exceed 7.0 μg m^{-3} over a large area in China, India, Western Europe, and Africa. More than 3.0 μg m^{-3} of TNO_3 is predicted over areas of Eastern and Western United States. In most areas, summer TNO_3 levels are lower than the corresponding winter values due to higher summer temperatures favoring partitioning to the shorter-lived gas-phase HNO_3. The heterogeneous $ClNO_2$ production decreases winter TNO_3 by 0.3-0.5 μg m^{-3} over much of China, India, Western Europe, and Western US. Although not visible in the figure, the heterogeneous $ClNO_2$ production decreases winter TNO_3 by as much as 2.0-3.0 μg m^{-3} at some locations in China. $ClNO_2$ formation can also increase winter TNO_3 due to recycled NO_x from $ClNO_2$ photolysis as well as enhanced HO levels which, in turn, enhance daytime production of HNO_3 via the homogeneous reaction of NO_2 + HO. In most locations, the reductions in nighttime heterogeneous production of HNO_3 outweigh the increases in the daytime homogeneous HNO_3 production and thus $ClNO_2$ chemistry reduces winter TNO_3 levels. However, in some isolated locations, $ClNO_2$ increases winter TNO_3 levels. The impact of $ClNO_2$ chemistry on summer TNO_3 is limited to much more localized areas in Europe, Africa, and China. $ClNO_2$ production decreases winter TNO_3 by 3.3% and summer TNO_3 by 0.3% averaged over the entire NH but by up to 25% and 7% in some locations.

3.3 Impact of the $ClNO_2$ production on ozone

The monthly mean of daily maximum 8-hr O_3 levels without the heterogeneous production of $ClNO_2$ and changes due to the $ClNO_2$ chemistry are shown in Figure 3. Ozone concentrations are highest in the summer near high population areas and are lower during winter over remote areas. Heterogeneous $ClNO_2$ formation chemistry enhances both the winter and summer O_3, however, the enhancements are greater in winter (>7.0 ppbv increase in monthly mean of 8-hr

daily maximum over a large area in China and 1.0-6.0 ppbv in the rest of the NH). $ClNO_2$ formation enhances summer O_3 by only 0.2-1.6 ppbv.

3.4 Impact on hydroxyl radical and subsequent impact on other chemical species

Heterogeneous $ClNO_2$ formation chemistry enhances both winter and summer HO levels. This chemistry increases winter HO by 3.5% and summer HO by 0.3% averaged over the entire NH. The increased HO can occur through several chemical pathways. First, as described in section 3.3, $ClNO_2$ enhances O_3 which in turn produces more singlet oxygen atom (O^1D) via photolysis. Additional O^1D leads to enhanced HO via its reaction with water vapor. Second, photolysis of $ClNO_2$ produces $Cl\cdot$ which subsequently oxidizes volatile organic compounds and, in turn, also leads to more HO. While on average winter HO is enhanced by 3.5%, larger increases occur in isolated areas. For example, winter HO over localized areas of China, Europe, United States, and Canada increases by more than 20% compared to the simulation without heterogeneous $ClNO_2$ formation chemistry. These findings are consistent with box model results constrained by measurements made in Los Angeles, CA which show $ClNO_2$ increasing morning HO levels by 25% [*Riedel et al.*, 2013].

Enhanced HO leads to increased secondary pollutants such as sulfate through the oxidation of sulfur dioxide. The monthly mean sulfate without the heterogeneous production of $ClNO_2$ and changes due to the $ClNO_2$ chemistry are shown in Figure 4. The inclusion of heterogeneous $ClNO_2$ formation chemistry enhances winter monthly sulfate by >0.35μg m^{-3} over China, >0.20 μg m^{-3} over India and Western Europe, and >0.05 μg m^{-3} over United States. This chemistry also enhances summer sulfate though its impact is smaller and more localized than in winter.

4. Discussion

To our knowledge, this is the first study that examines the impact of the heterogeneous $ClNO_2$ production on air quality across the Northern Hemisphere. Predicted $ClNO_2$ can reach high levels (in the range of 1 ppb) in several areas across the NH, especially during winter and can account for a sizeable fraction of the NO_Y budget. Due to the large grid size used for hemispheric modeling, we may not fully capture peak $ClNO_2$ concentrations and its effects on tropospheric chemistry; thus these modeling results may be considered a lower bound. Similar to previous modeling studies (*Simon et al.* [2009]; *Sarwar et al.* [2012]), this analysis shows that the resulting $ClNO_2$ alters air quality by decreasing total nitrate and enhancing O_3. Sizable $ClNO_2$ concentrations also increase HO which subsequently enhances the atmospheric oxidation capacity and secondary air pollutant formation. This work expands on previous studies by characterizing $ClNO_2$ concentrations and effects across many portions of the NH which have not previously been evaluated. We identify winter in China and Western Europe as the season and locations in which $ClNO_2$ chemistry is likely to have the largest impact. Much of the $ClNO_2$ predicted to span large inland areas of China forms as a result of chloride present in biomass burning plumes. While this is an intriguing finding, no field or lab studies have measured $ClNO_2$ formation on this type of particle. Previous studies focused on locations where chloride from sea salt and other sources was present in aqueous particles, while at least some of the chlorine in biomass burning particles may be in other forms (e.g. covalently bonded in organic chlorine compounds). These results highlight the need for further measurement studies to verify whether $ClNO_2$ forms on the surface of biomass burning particles and to quantify its impacts at the times and locations where the model predicts it is most important. It also underscores the need for developing a more accurate global emissions inventory for particulate chloride.

Disclaimer

Although this paper has been reviewed by EPA and approved for publication, it does not necessarily reflect EPA's policies or views.

Acknowledgements

The Community Multiscale Air Quality (CMAQ) model (CMAQv5.0.2) was used for generating the model results. The CMAQ model can be downloaded from http://www.cmascenter.org.

References

Appel, K. W., C. Chemel, S. J. Roselle, X. V. Francis, H. Rong-Ming, R. S. Sokhi, S. T. Rao, S. Galmarini (2012), Examination of the Community Multiscale Air Quality (CMAQ) Model Performance over the North American and European Domains, *Atmospheric Environment*, 53:142-155.

Appel, W., P. Bhave, A. Gilliland, G. Sarwar, S. J. Roselle (2008), Evaluation of the Community Multiscale Air Quality model version 4.5: uncertainties and sensitivities impacting model performance, Part II – Particulate Matter, *Atmospheric Environment*, 42:6057-6066.

Appel, K. W., A. B. Gilliland, G. Sarwar, and R.C. Gilliam (2007), Evaluation of the Community Multiscale Air Quality (CMAQ) model version 4.5: sensitivities impacting model performance, Part I - Ozone, *Atmospheric Environment*, 41, 9603–9615.

Bertram, T.H., J.A. Thornton, T.P. Riedel, A.M. Middlebrook, R. Bahreini, T.S. Bates, P.K. Quinn, D.J. Coffman (2009), Direct observations of N_2O_5 reactivity on ambient aerosol particles, *Goephysical Research Letters*, 36, L19803.

Bertram, T. H. and J. A. Thornton (2009), Toward a general parameterization of N2O5 reactivity on aqueous particles: the competing effects of particle liquid water, nitrate and chloride, *Atmospheric Chemistry and Physics*, 9, 8351–8363, doi:10.5194.

Binkowski, F. S. and S. J. Roselle (2003), Community Multiscale Air Quality (CMAQ) model aerosol component, I: Model description, *Journal of Geophysical Research*, 108, 4183, doi:10.1029/2001JD001409.

Byun, D. and K. L. Schere (2006), Review of the governing equations, computational algorithms, and other components of the Models-3 Community Multiscale Air Quality (CMAQ) modeling system, *Appl. Mech. Rev.*, 59, 51–77.

Davis, J. M., P. V. Bhave, and K. M. Foley (2008), Parameterization of N_2O_5 reaction probabilities on the surface of particles containing ammonium, sulfate, and nitrate, *Atmospheric Chemistry and Physics*, 8, 5295–5311, doi:10.5194.

Eder, B. and S. Yu (2006), A performance evaluation of the 2004 release of Models-3 CMAQ, *Atmospheric Environment*, 40, 4811-4824.

Eder, B. and S. Yu (2004), A performance evaluation of the 2004 release of Models-3 CMAQ, *Atmospheric Environment*, 40, 4811–4824.

Finlayson-Pitts, B.J., M.J. Ezell, J.N. Pitts Jr (1989), Formation of chemically active chlorine compounds by reactions of atmospheric NaCl particles with gaseous N_2O_5 and $ClONO_2$, *Nature*, 337(6204): 241-244.

Foley, K. M., S. J. Roselle, K. W. Appel, P.V. Bhave, J. E. Pleim, T. L. Otte, R. Mathur, G. Sarwar, J. Young, R.C. Gilliam, C. G. Nolte, J.T. Kelly, A. B. Gilliland, and J.O. Bash (2010), Incremental testing of the Community Multiscale Air Quality (CMAQ) modeling system version 4.7, *Geoscientific Model Development,* 3, 205–226, doi:10.5194.

Gong, S. L. (2003), A parameterization of sea salt aerosol source function for sub- and super-micronparticles, G*lobal Biogeochemical Cycles,* 17(4), 1097, doi: 10.1029/2003GB002079.

Kelly, J., P. Bhave, C.G. Nolte, U. Shankar, and K. Foley (2010), Simulating Emission and Chemical Evolution of Coarse Sea salt Particles in the Community Multiscale Air Quality (CMAQ) Model, *Geoscientific Model Development*, 3(1):257-273.

Kercher, J.P. (2009), Chlorine activation by N_2O_5: simultaneous, in situ detection of $ClNO_2$ and N_2O_5 by chemical ionization mass spectrometry, *Atmospheric Measurement Techniques*, 2, 193-204.

Leu, M.T. (1984), Kinetics of the reaction Cl + NO2 + M, *International Journal of Chemical Kinetics*, 16(11): 1311-1319.

366 Lobert, J.M., W.C. Kenee, J.A. Logan, R. Yevich (1999), Global chlorine emissions from
367 biomass burning: reactive chlorine emissions inventory, J. *Geophysical Research*, 104, D7,
368 8373-8389.
369 Mathur, R., S. Roselle, J. Young, and D. Kang (2013), Representing the Effects of Long-Range
370 Transport and Lateral Boundary Conditions in Regional Air Pollution Models, Chapter 51,
371 Air Pollution Modeling and its Application XXII. Springer, Heidelburg, Germany,
372 2014:303-308.
373 Mathur, R., R. C. Gilliam, R. Bullock, S. J. Roselle, J. E. Pleim, D. C. Wong, F. S. Binkowski,
374 and D. G. Streets (2011), Extending the Applicability of the Community Multiscale Air
375 Quality Model to Hemispheric Scales: Motivation, Challenges, and Progress, Chapter 30,
376 Douw G. Steyn & Silvia TriniGastelli (ed.), NATO/SPS/ITM Air Pollution Modeling and
377 its Application XXI. Springer Netherlands, Netherlands, C Series: 175-179.
378 Mielke, L.H, J. Stutz, C. Tsai, S.C. Hurlock, J.M. Roberts, P.R. Veres, K.D. Froyd, P.L. Hayes,
379 M.J. Cubison, J.L. Jimenez, R.A. Washenfelder, C.J. Young, J.B. Gilman, A.D. Gouw, J.H.
380 Flynn, N. Grossberg, B.L. Lefer, J. Liu, R.J. Weber, H.D. Osthoff (2013), Heterogeneous
381 formation of nitryl chloride and its role as a nocturnal NO_x reservoir species during CalNex-
382 LA 2010*, J. Geophysical Research: Atmospheres*, 118, 10638-10652.
383 Mielke, L. H., A. Furgeson, and H.D. Osthoff (2011) Observation of $ClNO_2$ in a mid-
384 continental urban environment, *Environmental Science &Technology*, 45, 8889–8896.
385 Osthoff, H. D., J.M. Roberts, A.R. Ravishankara, E.J. Williams, B.M. Lerner, R. Sommariva,
386 T.S. Bates, D. Coffman, P.K. Quinn, J.E. Dibb, H. Stark, J.B. Burkholder, R.K. Talukdar,
387 J. M. Meagher, F. C. Fehsenfeld, and S.S. Brown (2008), High levels of nitryl chloride in
388 the polluted subtropical marine boundary layer, *Nature Geoscience*, 1, 324–328.
389 Philips, G.J., M.J. Tang, J., Thieser, B. Brickwedde, G. Schuster, B. Bohn, J. Lelieveld, and
390 J.N. Crowley (2012), Significant concentrations of nitryl chloride observed in rural

391 continental Europe associated with the influence of sea salt chloride and anthropogenic
392 emissions, *Geophysical Research Letters*, 39, L10811, doi:10.1029/2012GL051912.
393 Reff, A., Bhave, P. V., Simon, H., Pace, T. G., Pouliot, G. A., Mobley, J. D., and Houyoux, M.
394 (2009), Emissions inventory of $PM_{2.5}$ trace elements across the United States, Environ.
395 Science & Technology, 43, 5790–5796.Riedel, T.P., T.H. Bertram, T.A. Crisp, E.J.
396 Williams, B.M. Lerner, A. Blasenko, S.M. Li, J. Gilman, J.D. Gouw, D.M. Bon, S.S.
397 Brown, and J. A. Thornton (2012), Nitryl chloride and molecular chlorine in the coastal
398 marine boundary layer, *Environmental Science & Technology*, 46, 10463-10470.
399 Riedel, T.P., N.L. Wagner, W.P. Dube, A.M. Middlebrook, C.J. Young, F. Ozturk, R. Bahreini,
400 T.C. VandenBoer, D.E. Wolfe, E.J. Williams, J.M. Roberts, S.S. Brown, and J.A. Thornton
401 (2013), Chlorine activation within urban or power plant plumes: vertically resolved $ClNO_2$
402 and Cl_2 measurements from a tall tower in a polluted continental setting, *Journal of*
403 *Geophysical Research: Atmospheres*, 118, 8702-8715.
404 Roberts, J. M., H.D. Osthoff, S.S. Brown, A.R. Ravishankara, D. Coffman, P. Quinn, and T.
405 Bates (2009), Laboratory studies of products of N2O5 uptake on Cl- containing substrates,
406 *Geophysical Research Letter*, 36, L20808, doi:10.1029/2009GL040448.
407 Sarwar, G., H. Simon, K. Fahey, R. Mathur, W.S. Goliff, and W. R. Stockwell (2014), Impact
408 of sulfur dioxide oxidation by Stabilized Criegee Intermediate on sulfate, *Atmospheric*
409 *Environment,* 85, 204-214.
410 Sarwar, G., J. Godowitch, B. H. Henderson, K. Fahey, G. Pouliot, W.T. Hutzell, R. Mathur,
411 D. Kang, W. S. Goliff, and W. R. Stockwell (2013), A comparison of atmospheric
412 composition using the Carbon Bond and Regional Atmospheric Chemistry Mechanisms,
413 *Atmospheric Chemistry and Physics,* 13, 9695-9712**.**

414 Sarwar, G., H. Simon, P. Bhave, G. Yarwood (2012), Examining the impact of heterogeneous
415 nitryl chloride production on air quality across the United States, *Atmospheric Chemistry*
416 *and Physics*, 12, 1-19.
417 Sarwar, G., D. Luecken, G. Yarwood, G. Whitten, B. Carter (2008), Impact of an updated
418 Carbon Bond mechanism on air quality using the Community Multiscale Air Quality
419 modeling system: preliminary assessment, *Journal of Applied Meteorology and*
420 *Climatology*, 47, 3-14.
421 Simon, H., Y. Kimura, G. McGaughey, D.T. Allen, S.S. Brown, H.D. Osthoff, J.M. Roberts,
422 D. Byun, and D. Lee (2009), Modeling the impact of ClNO2 on ozone formation in the
423 Houston area, *Journal of Geophysical Research* 114, D00F03,
424 doi:10.1029/2008JD010732.
425 Simon, H., Y. Kimura, G. McGaughey, D.T. Allen, S.S. Brown, D. Coffman, J. Dibb., H.D.
426 Osthoff, P. Quinn, J.M. Roberts, G. Yarwood, S. Kemball-Cook, D. Byun, D. Lee (2010),
427 Modeling heterogeneous $ClNO_2$ formation, chloride availability, and chlorine cycling in
428 Southeast Texas, *Atmospheric Environment*, 44, 5476-5488.
429 Skamarock, W. C., J.B. Klemp, J. Dudhia, D.O. Grill, D.M. Barker, M.G. Duda, X-Y, Huang,
430 W. Wang, and J.G. Powers, (2008), A description of the advanced research WRF version
431 3. NCAR Tech Note NCAR/TN 475 STR, 125 pp. [Available from UCAR
432 Communications, P.O. Box 3000, Boulder, CO 80307.]
433 Thornton, J. A., J.P. Kercher, T.P. Riedel, N.L. Wagner, J. Cozic, J.S. Holloway, W.P. Dube,
434 G.M. Wolfe, P.K. Quinn, A.M. Middlebrook, B. Alexander, and S.S. Brown (2010), A
435 large atomic chlorine source inferred from mid-continental reactive nitrogen chemistry,
436 *Nature*, 464, 271–274.

Whitten, G. Z., G. Heo., Y. Kimura, E. McDonald-Buller, D.T. Allen, W.P.L. Carter, and G. Yarwood (2010), A new condensed toluene mechanism for Carbon Bond: CB05-TU, *Atmospheric Environment*, 44, 5346–5355.

Young, C.J., R.A. Washenfelder, J.M. Roberts, L.H. Mielke, H.D. Osthoff, C. Tsai, O., Pikelynaya, J., Stutz, P.R. Veres, A.K. Cochran, T.C. VandenBoer, J. Flynn, N., Grossberg, C.L. Haman, B. Lefer, H. Stark, M. Graus, J. de Gouw, J.B. Gilman, W.C. Kuster, S.S. Brown (2012), Vertically resolved measurements of nighttime radical reservoirs in Los Angeles and their Contribution ot the urban radical budget, *Environmental Science and Technology*, 46, 10965-10973.

Yu, S., R. Dennis, S. Roselle, A. Nenes, J. Walker, B. Eder, K. Schere, J. Swall, W. Malm, and W. Robarge (2005), An assessment of the ability of three-dimensional air quality models with current thermodynamic equilibrium models to predict aerosol NO_3–, *Journal of Geophysical Research*, 110, D07S13.

Table 1: A comparison of predicted $ClNO_2$ concentrations to observed data

Location	Date	Peak observation (pptv)	Peak predictions (pptv)		Ref.
			January	June	
Houston, TX, USA	Aug-Sep 2008	1,200	1,100	150	Osthoff et al., [2008]
Boulder, CO, USA	Feb 2009	450	400	70	Thornton et al., [2010]
Boulder, CO, USA	Feb-Mar 2011	1,300	400	70	Reidel et al., [[2013]
Los Angeles, CA, USA (marine)	May-Jun 2010	2,100	2,300	600	Reidel et al., [2012]
Pasadena, CA, US (inland)	May-Jun 2010	3,600	1,600	700	Mielke et al., [2013]
Long Island Sound	Mar 2008	200	1,300	1,400	Kercher et al., [2009]
North Atlantic	Mar 2008	100	2,100	600	Kercher et al., [2009]
Calgary, Alberta, Canada	Apr 2010	250	300	30	Mielke et al., [2011]
Frankfurt, Germany	Aug-Sep 2011	800	1,300	800	Philips et al., [2013]

Note: Observed and model values are not paired in time and space. Model predictions are taken from the general geographic areas of observed data.

Figures

Figure 1: (a) Mean of nightly 1-h maximum $ClNO_2$ in January without the heterogeneous $ClNO_2$ production (pptv) (b) mean of nightly 1-h maximum $ClNO_2$ in June without the heterogeneous $ClNO_2$ production (pptv) (c) mean of nightly 1-h maximum $ClNO_2$ in January with the heterogeneous $ClNO_2$ production (ppbv) (d) mean of nightly 1-h maximum $ClNO_2$ in June with the heterogeneous $ClNO_2$ production (ppbv). Note that scales for panels a) and b) are given in units of pptv while scales in panels c) and d) are given in unites of ppbv.

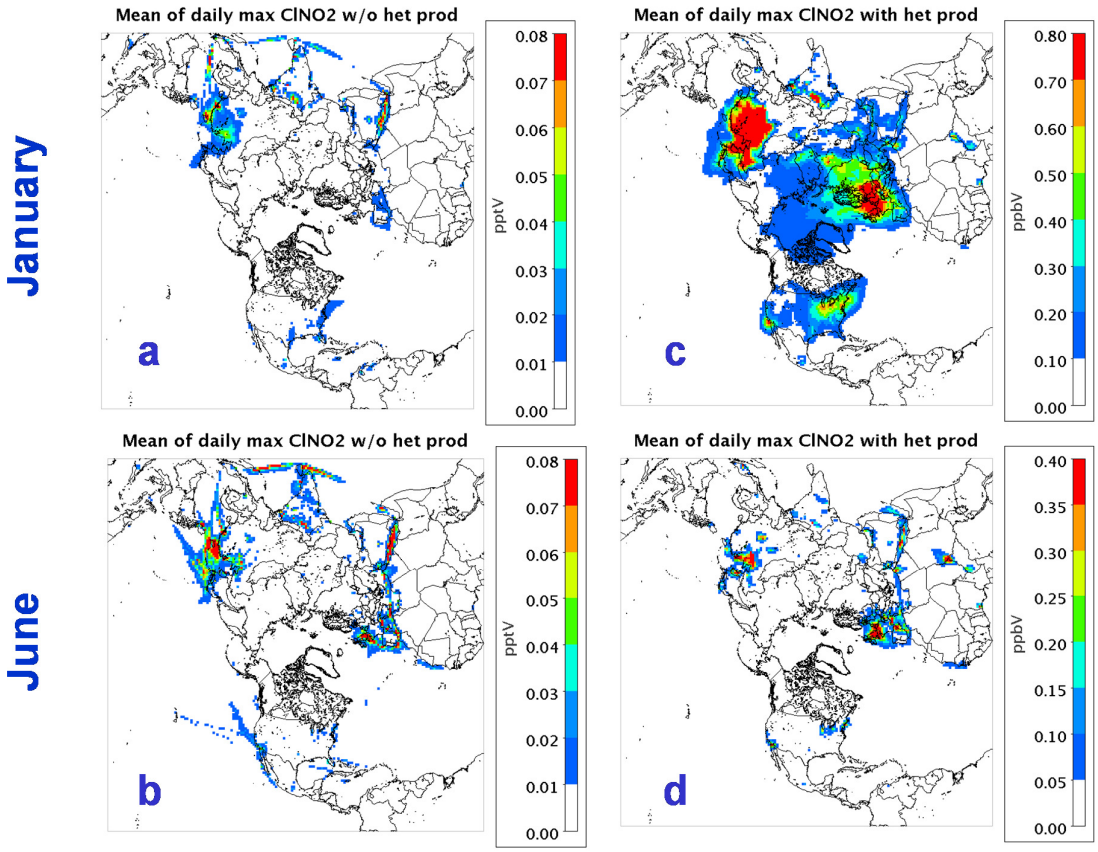

Figure 2**:** (a) Mean TNO_3 in January without the heterogeneous $ClNO_2$ production (b) mean TNO_3 in June without the heterogeneous $ClNO_2$ production (c) changes in mean TNO_3 in January due to the heterogeneous $ClNO_2$ production (c) changes in mean TNO_3 in June due to the heterogeneous $ClNO_2$ production

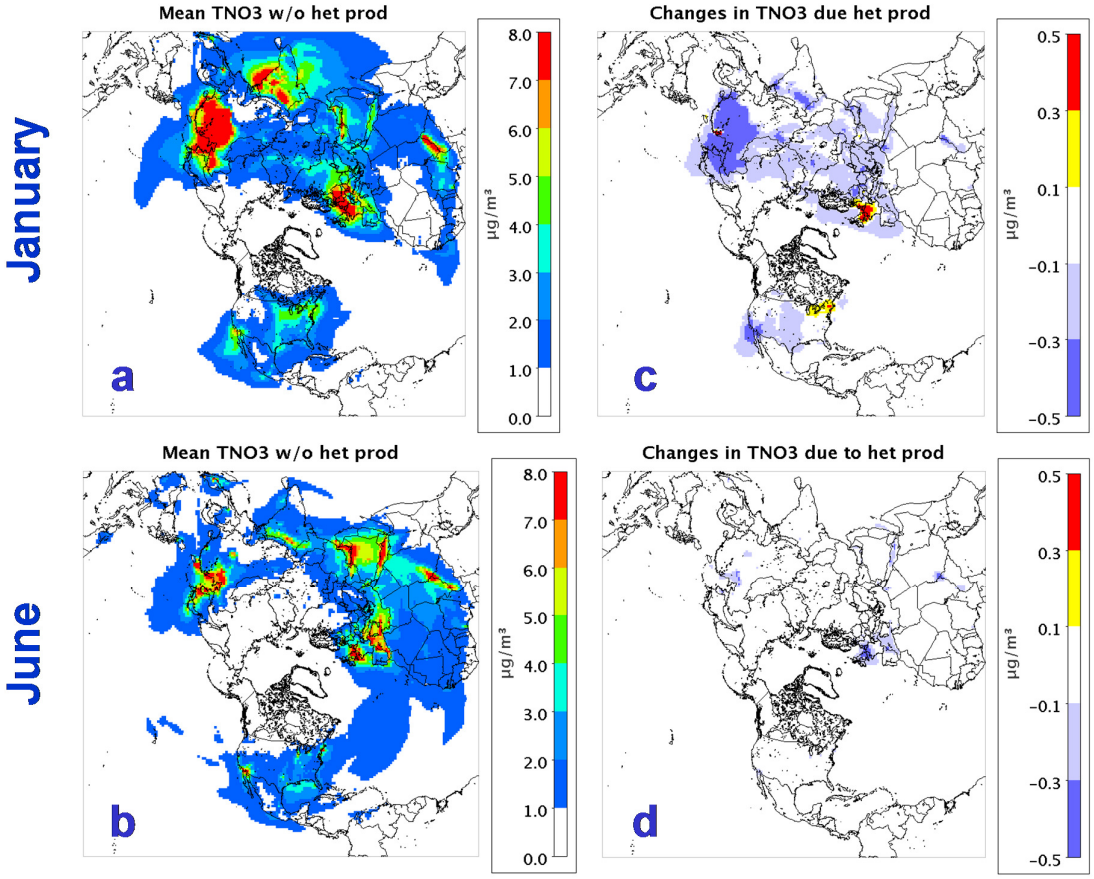

Figure 3**:** (a) Mean of daily maximum 8-hr O_3 in January without the heterogeneous $ClNO_2$ production (b) mean of daily maximum 8-hr O_3 in June without the heterogeneous $ClNO_2$ production (c) changes in mean daily maximum 8-hr O_3 in January due to the heterogeneous $ClNO_2$ production (d) changes in mean daily maximum 8-hr O_3 in June due to the heterogeneous $ClNO_2$ production

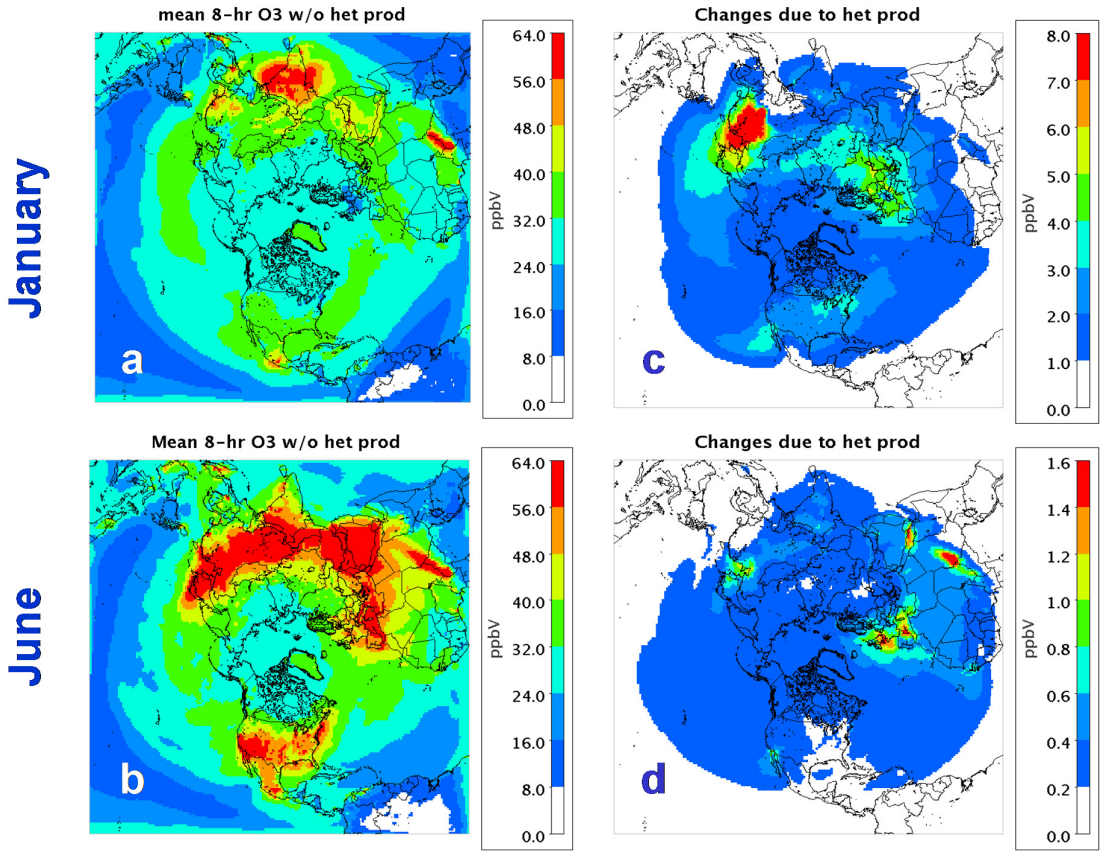

Figure 4: (a) Mean sulfate in January without the heterogeneous $ClNO_2$ production (b) mean sulfate in June without the heterogeneous $ClNO_2$ production (c) changes in mean sulfate in January due to the heterogeneous $ClNO_2$ production (d) changes in mean sulfate in June due to the heterogeneous $ClNO_2$ production